Nonradiative recombination processes in nickel- and iron-doped ZnS and ZnSe studied by photoinduced electron-spin resonance

M. Surma, A. J. Zakrzewski, and M. Godlewski
Institute of Physics, Polish Academy of Sciences, 02-668 Warsaw, Al. Lotników 32/46, Poland
(Received 21 February 1995; revised manuscript received 28 June 1995)

The results of electron-spin resonance experiments on nickel- and/or iron-doped ZnS and ZnSe are presented. The position of the $Ni^{1+/2+}$ energy level in the band gap of ZnS and ZnSe is determined. A good agreement with some of the previous estimations is found. The role of nickel and iron impurities in nonradiative recombination processes in ZnS and ZnSe is discussed. The present results indicate that the three-center Auger recombination process limits the efficiency of a radiative decay of donor-acceptor pairs in both ZnS and ZnSe.

INTRODUCTION

Transition-metal (TM) impurities such as iron and chromium are known to be very effective deactivators (killers) of the visible photoluminescence (PL) coming from the radiative recombination of donor-acceptor pairs (DAP's) in ZnS (Refs. 1 and 2) and ZnSe compounds. Their role in nonradiative recombination transitions was related to the bypassing process[3] (free electrons and holes recombine via a TM impurity level instead of populating DAP's); the formation of complex centers composed of an activator and a deactivator of the emission, e.g., copper-iron pairs;[2,4] and energy-transfer processes from donor-acceptor pairs to nearby TM ions. We have shown recently that for the iron impurity in ZnS the energy-transfer process is of an Auger type [three-center Auger recombination[5,6] (TCAR)], i.e., that iron is ionized in the process of energy transfer from DAP's.

The efficiency of the different nonradiative recombination processes depends on the relative concentrations of PL activators and deactivators, on their carrier trapping rates and, for the TCAR process, on the ionization cross section of the TM ion. Thus it may differ for each TM ion and also from sample to sample.[1,2] The latter explains the slow progress in the understanding of nonradiative recombination processes in semiconductor phosphors. Our previous studies of iron- and chromium-doped ZnS indicated that the bypassing mechanism is dominant, with some contribution of the TCAR process.[1,2] It was also shown that the bypassing process can be important for complex centers, consisting of a PL activator and PL deactivator.

In this paper we present results of photoinduced electron-spin resonance (photo-ESR) studies of nickel- and iron-doped ZnS and ZnSe bulk samples. The photoexcitation and photoquenching spectra of the ESR signals were measured. Based on the results, the dominant channels of nonradiative recombination via these two TM ions in ZnS and ZnSe are discussed. Electron and hole capture rates for nickel and iron impurities are compared. Previous estimations of the position of Ni^{1+} energy level in the band gap of ZnS and ZnSe are verified.

EXPERIMENTAL PROCEDURE

ZnSe and ZnS crystals were grown by the Bridgman technique. They were intentionally doped with nickel to the level between 5×10^{17} and 1×10^{19} cm^{-3}. Iron, chromium, copper, and manganese were found to be common contaminants of all the crystals studied. Their ESR signals were also observed in undoped crystals. Some of the crystals studied were codoped with aluminum. Iron- and chromium-doped or codoped crystals were also studied for comparison.

The ESR and photo-ESR experiments were performed on a conventional *X*-band ESR spectrometer (Bruker 418s). High-pressure mercury and halogen lamps with Carl-Zeiss Jena interference filters were used for selective optical excitation. The samples were mounted in a helium gas flow cryostat working in the temperature range of 4–300 K with a temperature stability of about 0.5 K.

RESULTS

The ESR signal of manganese Mn^{2+} was observed before, after, and under illumination of all ZnS and ZnSe samples studied. This signal was not photosensitive. Furthermore four other ESR signals were found in different ZnS crystals studied. These signals were observed only under illumination in a particular spectral range. Three of the signals were isotropic and had *g* factors of 1.4, 1.999, and 2.003, respectively. The latter two ($g=1.999$ and 2.003) are assigned to Cr^{+} and Fe^{3+} ions in ZnS, based on previous ESR and photo-ESR measurements.[7,8] The magnetic resonance with a *g* factor of about 1.4 is related to Ni^{+}.[9] This signal was found only in nickel-doped crystals. The fourth signal, with a *g* factor of 2.248, was slightly anisotropic and was observed in some of the ZnS crystals studied. This ESR signal may be tentatively attributed to the previously observed ESR signal of Fe^{+}.[10]

No nickel-related ESR signal was observed in ZnSe, irrespective of the sample, energy of illumination, and temperature of the measurement. The only ESR signal detected upon photoexcitation was due to Fe^{3+}

0163-1829/95/52(16)/11879(5)/$06.00

($g=2.045$). The photoexcited signal of Fe^{3+} decayed slowly after the light was turned off at low temperature (e.g., 20 s at 5 K), which allowed us to perform photoquenching measurements in addition to photoexcitation studies.

The spectral dependence of the photoexcitation of the ESR signals was measured in the following way. After the saturation value of the signal amplitude was measured, the light was turned off and the ESR signal was quenched to zero, either by applying a second illumination of an appropriate energy or by raising the temperature. This procedure was repeated for each of the excitation energies selected in order to keep the same initial conditions.[11] The spectral resolution of that experiment was determined by the bandwidths of the high transmittance interference filters used. The spectral dependencies of the saturation amplitudes of Ni^{1+} and Fe^{3+} ESR signals in ZnS are presented in Fig. 1. In a similar manner, the spectral dependencies of the rise and decay rates of the ESR signal upon the illumination[11] were measured. The results for the Fe^{3+} ESR signal in ZnSe are shown in Fig. 2.

Spectral dependencies, similar to those shown in Figs. 1 and 2, were observed for all iron- and nickel-doped ZnS and ZnSe samples investigated. Only some changes in the intensities of different bands from sample to sample were found, which could be related to the doping level. The results for Cr only and Cr- and Fe-doped samples were in agreement with those reported previously,[2,12–14] and thus will not be discussed here. We underline, however, that without detailed ESR studies performed for differently doped ZnS and ZnSe samples, an unambiguous identification all the photo-ESR bands shown in Figs. 1 and 2 would be impossible.

DISCUSSION

The ground state of Fe^{2+} is a spin singlet and does not give rise to any ESR signal. The Fe^{3+} resonance was observed only upon illumination. A light-induced population of the Fe^{3+} state can be achieved only if Fe^{2+} is directly ionized or if it changes its charge state by trapping a free hole ($Fe^{2+}+h_{VB}->Fe^{3+}$, where h_{VB} is the hole in the valence band). Simultaneously, direct neutralization of the Fe^{3+} state and free-electron trapping ($Fe^{3+}+e_{CB}->Fe^{2+}$, where e_{CB} is the electron in the conduction band) have to be considered. In the carrier trapping process the change of the Fe^{3+} ESR signal intensity reflects the ionization processes of other centers. For this reason we could study the ionization transitions of the nickel impurity in ZnSe even though the Ni-related signal was not directly observed. One should also bear in mind that there is a fundamental difference between an optical absorption and a photo-ESR study. To observe the light-induced change in the intensity of a given ESR signal, the change of the center concentration must be

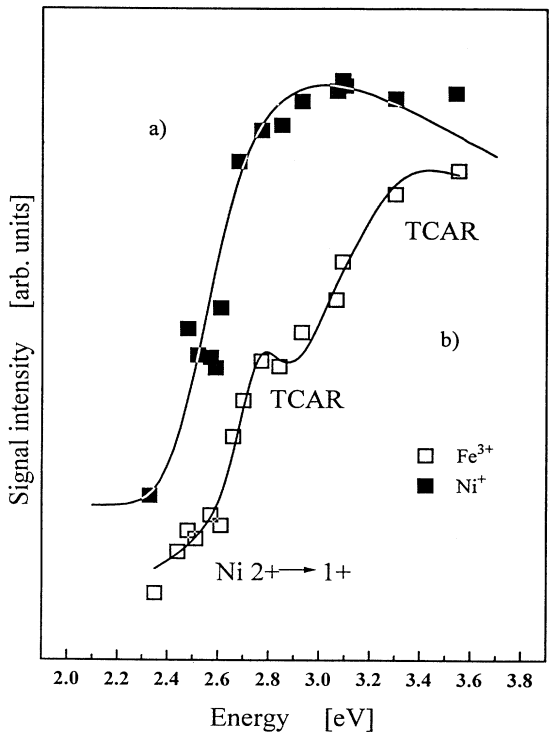

FIG. 1. Spectral dependencies of the photoexcitation of (a) Ni^{+} and (b) Fe^{3+} ESR signals in ZnS. The solid line in (a) represents the theoretical fit to the experimental results with the formula, which takes into account the lattice relaxation accompanying the change of the charge state of the ion.

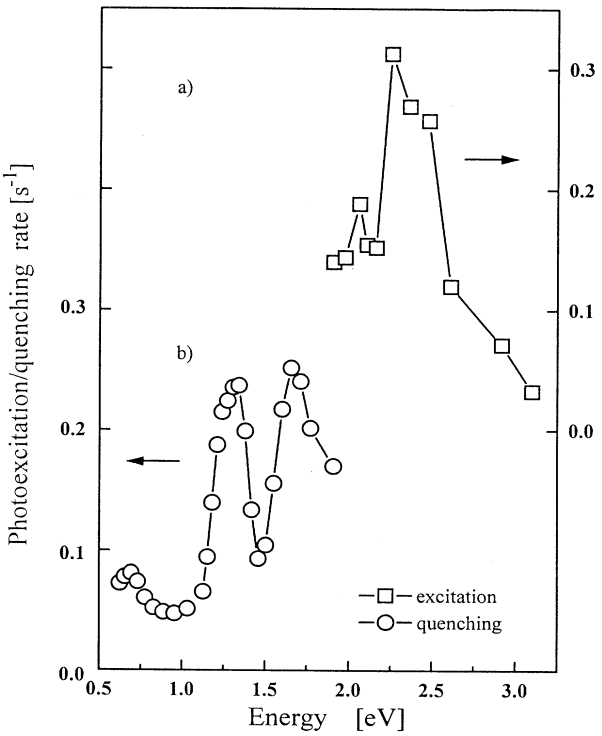

FIG. 2. Spectral dependencies $[\tau^{-1}(h\nu)]$ of the rise (a) and decay (b) times (τ) of the Fe^{3+} ESR in the ZnSe lattice upon different illuminations.

greater than the ESR detection limit. A simple estimation shows that the lifetime of the photoexcited state should be longer than approximately 1 ms,[11] which means that fast retrapping of ionized carriers can prevent detection of the signal photosensitivity. A nearly metastable change of the center charge state is necessary in the photo-ESR study.[11]

The lifetime of the photoexcited state is determined by the competition of two processes: (a) retrapping of the free carriers by the ionized center, and (b) capturing of the photogenerated carriers by other trap centers. A long lifetime of the photoexcited ESR signal thus means that the retrapping is not efficient. The efficiency of the second process depends not only on the concentration of competing trap centers but also on their carrier capture cross sections. This is why the photo-ESR experiment also yields information on carrier capture processes. Moreover, trapping of free carriers by TM ions reduces the number of electron-hole pairs populating donor and acceptor centers, and thus deactivates the visible PL of DAP's in ZnS and ZnSe. Consequently, a photo-ESR study yields information on the role of a given TM ion in the deactivation processes of the DAP PL.

ZnS

Photosensitive ESR signals of Fe^{3+} and Ni^{1+} were observed in ZnS samples doped with nickel and iron. In the spectral dependence of the photoexcitation of the Ni^{1+} ESR signal, shown in Fig. 1(a), a single band starting at about 2.4 eV is visible. As discussed above, one of the processes which can populate the Ni^{1+} energy level is the capture of photogenerated free electrons by Ni^{2+} ions. The second is the direct or indirect (e.g., due to the TCAR process) photoionization of nickel, i.e., $Ni^{2+}+h\nu \rightarrow Ni^{1+}+h_{VB}$. There is no chance to distinguish which of the two alternative mechanisms is responsible for the creation of the Ni^{1+} charge state based on results of one ESR study only. However, it becomes possible when the ionization transitions of other deep centers residing in the investigated material are known. Ionization transitions of Cr, Fe, and common acceptors were resolved in previous ESR studies of chromium-, iron-, and copper-doped ZnS.[2,12,15] They occur at energies slightly different from the transition observed in the Ni-doped sample. For this reason we assign the observed photo-ESR band to the direct ionization transition of Ni ($Ni^{2+}+h\nu -> Ni^{1+}+h_{VB}$). At energies higher than 2.6 eV, deep acceptor centers of ZnS are also ionized. If the photogenerated free electrons are trapped by Ni^{2+}, it may increase the amplitude of the photoexcited Ni^{1+} ESR. The photoexcitation of the Ni^{1+} ESR signal can, thus, be explained as follows: (a) At excitation energies in the range of 2.4–2.6 eV, the direct ionization of nickel is observed. (b) At energies higher than 2.6 eV; Ni^{1+} may also be generated due to capture of electrons ionized to the CB from deep acceptors (Cu-D, *A* centers) of ZnS. Consequently, we can locate the 1+/2+ energy level of nickel at about 2.4 eV above the VB in the band gap of ZnS, which is in good agreement with some previous estimations.[16] The energy value of 2.4 eV corresponds to the thermal ionization energy (E_{th}). 2.6 eV (optical ionization energy E_{opt}) was obtained by fitting the experimental results with a formula:

$$\sigma=\frac{1}{\sqrt{\pi}}\int_{-\beta}^{+\infty}\sigma_{el}(E_{opt},h\nu+\Gamma/z)(1+\Gamma/z)^{-1}e^{-z^2}dz\ ,$$

$$\beta=\frac{h\nu-E_{opt}}{\Gamma}\ ,$$

$$\Gamma=\frac{\omega_0}{\omega_{exc}}\left[2(E_{opt}-E_{th})\hbar\omega_0\coth\frac{\hbar\omega_0}{2kT}\right]^{1/2}\ ,$$

$$\sigma_{el}(E_{opt},h\nu)\approx(h\nu)^{-3}\sqrt{h\nu-E_{opt}}\ ,$$

where E_{opt}, E_{th}, and Γ are the ionization parameters of the center, and ω_0 and ω_{exc} are frequencies of phonons coupled to the ground and charge-excited states of the ion. The above formula takes into account coupling to the lattice vibrations, since the spectrum observed is a convolution of both electronic and vibronic transitions.

Further details on the fitting procedure used can be found elsewhere.[11,17] In the fit we have assumed that the direct ionization transition dominates over the indirect processes in the whole spectral range, which is rather arbitrary. However, it is supported by the fact that the photo-ESR spectrum clearly has a one-band character, which indicates that the indirect process is not efficient in the Ni^{1+} photoexcitation. The same fit also yields the value of the lattice relaxation energy ($E_{opt}-E_{th}$, about 0.2 eV), which results from an increase of the ion-ligand distance induced by the change of the nickel charge state.[11,18]

In Fig. 3 we compare the light-induced amplitudes of the Fe^{3+} ESR signal measured for iron- (lower curve) and nickel- (upper curve) doped ZnS samples. The higher-energy part of the Fe^{3+} photoexcitation spectrum in ZnS:Fe was explained by the TCAR processes.[5,6] The initial step in the TCAR process is the ionization of a deep acceptor, which is followed by trapping of the photogenerated electrons by shallow donors. The populated donor-acceptor pairs recombines and the energy is transferred to the nearby TM ion.[5,6] A similar process is observed in the excitation spectrum of the Fe^{3+} ESR signal in Ni codoped samples for photon energies larger than 2.6 eV. In addition, a distinct band occurs starting at 2.4 eV (see Fig. 3). Its spectral position coincides with the Ni ionization band and thus we attribute the excitation band to an indirect process in which the free holes generated in the photoionization transition of Ni^{2+} are captured by iron ions. The energy-level position of the nickel 1+/2+ state in the band gap of ZnS can thus also be derived from the behavior of the photosensitive Fe^{3+} ESR signal.

In the TCAR process, the Fe^{3+} ESR signal is excited due to nonradiative decay of a photoexcited donor acceptor pair[2] (the DAP decays nonradiatively and its recombination energy is transferred to a nearby Fe^{2+} center, which is ionized). The importance of such a process was first proven for the Fe ions in ZnS crystals.[5,6] It remained an open question if the TCAR process can be also efficient for other TM ions and in lattices other than ZnS.

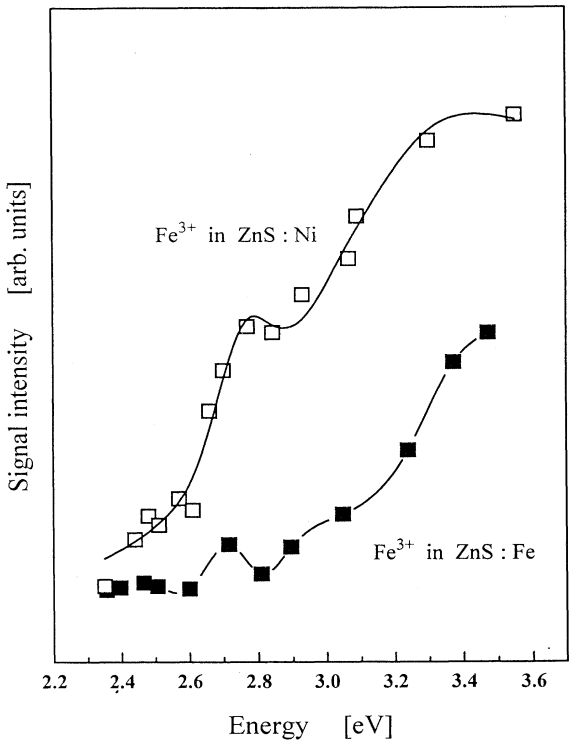

FIG. 3. Spectral dependencies of the photoexcitation of the Fe^{3+} ESR signal in nickel- (upper curve) and iron- (lower curve) doped ZnS.

The main difficulty in identifying the TCAR transition stems from the fact that the ionization transition of a TM ion is usually followed by the appearance of its intrashell PL emission only. Free carriers ionized from the TM ion are retrapped via one of the excited intrashell states of the ion, as was observed for, e.g., Fe ions in ZnS and ZnSe.[4,19] The intrashell PL emission of the ion is then observed.

In previously reported ESR experiments, the TCAR process was observed for ZnSe:Fe crystals codoped with chromium. Chromium in ZnS is an efficient electron trap center and traps some of the electrons ionized from the Fe centers. In this way the process could be detected in the ESR study. Figure 1 shows strong TCAR photoexcitation bands of the Fe^{3+} ESR in Ni-doped ZnS samples. We can conclude, hence, that nickel can efficiently trap free electrons ionized from Fe centers to the CB, i.e., the bypassing process can be efficient for the nickel ion in ZnS, which agrees with previous estimations.[3]

The low-energy band in the Fe^{3+} excitation spectrum (Fig. 1) can be attributed to the direct ionization transition of nickel. A fraction of the photogenerated holes in the Ni ionization transition can be trapped by iron Fe^{2+} centers, leading to an appearance of the Fe^{3+} ESR signal. The hole trapping by Fe ions is most probably responsible for the lack of the Ni^{3+} resonance in our ESR study, and indicates that Fe^{2+} ions can compete with Ni^{2+} ions in the trapping of free holes. Since the Ni concentration was larger than that of iron, we conclude that the capture cross sections are larger for Fe than for Ni. However, for both of these TM ions the bypassing process (free-carrier recombination via the TM center) should be efficient.

ZnSe

Only the Mn^{2+} ESR was observed prior to illumination in the nickel-doped ZnSe. A relatively weak ESR signal of Fe^{3+} was created upon illumination with 1.9–3.0-eV photon energies. The spectral dependence of the ESR signal is presented in Fig. 2(a). The photo-ESR spectrum differs from that observed by us for ZnSe intentionally doped with iron. The dominant excitation band visible for photon energies above 2.1 eV was not observed in the Fe-doped sample. It must be related to some indirect excitation process, and we attribute the band to the ionization transitions of deep acceptor centers of ZnSe, identified in previous optically detected magnetic resonance (ODMR) studies.[20] After comparing the results obtained for different ZnSe samples we can conclude that in Ni-doped ZnSe an efficient excitation of the Fe^{3+} ESR occurs only when ZnSe acceptors are ionized. As in such ionization transitions, free electrons are photogenerated, and their trapping by Fe^{3+} should lead to a photoquenching of the ESR signal instead of the observed photoexcitation. As discussed above, the photoexcitation spectrum of the Fe^{3+} ion in ZnS:Ni was dominated by the TCAR processes; i.e., it reflected the excitation spectrum of DAP PL, which is related to the ionization of deep acceptor centers of ZnS. By analogy, we propose that the TCAR process leads to Fe^{3+} photoexcitation for photon energies larger than 2.1 eV. Some of the free electrons are trapped by shallow donors and nickel ions rather than by Fe centers. The first process populates DAP's and promotes their radiative and nonradiative (the TCAR process) recombination. Even though the above interpretation is still ambiguous, this is an indication that TCAR processes might be efficient in the ZnSe lattice. We can also conclude that the electron-capture rate by nickel in ZnSe must be quite large. Otherwise, as explained above, we should not observe the TCAR process via an excitation of the Fe^{3+} ESR signal.

The photoquenching of the Fe^{3+} ESR signal starts at about 1.1 eV, which was not observed for iron-doped ZnSe. Also, a weak band visible in the low-energy part of the photoexcitation spectrum for nickel-doped samples was not observed in other samples. We attribute these two bands to two complementary nickel ionization transitions: $Ni^{1+}+h\nu \rightarrow Ni^{2+}+e_{CB}$ (photoquenching) and $Ni^{2+}+h\nu \rightarrow Ni^{1+}+h_{VB}$ (photoexcitation). From the theoretical fit to the ESR results we estimate the energy level of $Ni^{1+/2+}$ to be positioned 1.1 eV below the conduction band of ZnSe. This location agrees well with the one determined from some previous optical investigations.[21]

CONCLUSIONS

Photo-ESR measurements allow us to verify the previous estimations of the position of the $Ni^{1+/2+}$ energy level in the band gap of ZnS and ZnSe crystals. The ESR study shows that in both these materials nickel is a very efficient electron trap center, which indicates its destruc-

tive role in nonradiative recombination of electron-hole pairs. This is due to the so-called bypassing process, expected by us to be very efficient. The important observation reported in the present study is the observation of the three-center Auger processes for the iron ion in the ZnSe lattice. We show that, similar to the cases for iron and chromium in ZnS, iron in ZnSe deactivates the visible DAP emission due to the Auger-type three-center energy-transfer transitions. Such a process, together with the bypassing process, accounts for the high efficiency of the nonradiative processes in iron- and/or nickel-doped (contamined) ZnS and ZnSe crystals.

[1]M. Godlewski and M. Skowroński, Phys. Rev. B **32**, 4007 (1985).
[2]M. Godlewski and A. Zakrzewski, in *II-VI Semiconductor Compounds,* edited by M. Jain (World Scientific, Singapore, 1993), p. 205.
[3]M. Tabei, S. Shionoya, and H. Ohmatsu, Jpn. J. Appl. Phys. **14**, 240 (1976).
[4]M. Godlewski, Solid State Commun. **47**, 811 (1983).
[5]A. Zakrzewski and M. Godlewski, Phys. Rev. B **34**, 8993 (1986).
[6]M. Godlewski, A. Zakrzewski, and M. Z. Cieplak, in *Defects in Semiconductors,* Proceedings of the 14th International Conference on Defects in Semiconductors, Paris, 1986, edited by H. J. von Bardeleben (Trans Tech, Switzerland, 1986) [Mater. Sci. Formu **10-12**, 487 (1986)].
[7]J. Dieleman, R. S. Title, and W. V. Smith, Phys. Lett. **1**, 334 (1962).
[8]R. S. Title, Phys. Rev. **131**, 623 (1963).
[9]M. Schulz and G. G. Wepfer, Solid State Commun. **10**, 405 (1972).
[10]W. C. Holton, J. Schneider, and T. L. Estle, Phys. Rev. **133**, A1638 (1964).
[11]M. Godlewski, Phys. Status Solid A **91**, 11 (1985).
[12]M. Godlewski, J. Appl. Phys. **56**, 2901 (1984).
[13]M. Godlewski and M. Kamińska, J. Phys. C **13**, 6537 (1980).
[14]M. Surma, M. Godlewski, and T. Surkova, Phys. Rev. B **50**, 8319 (1994).
[15]M. Godlewski, W. E. Lamb, and B. C. Cavenett, J. Phys. C **15**, 3925 (1982).
[16]J. M. Noras and J. W. Allen, J. Phys. C **13**, 3511 (1980).
[17]U. Piekara, J. M. Langer, and B. Krukowska-Fulde, Solid State Commun. **23**, 583 (1977).
[18]M. Godlewski, J. Appl. Phys. **59**, 466 (1986).
[19]K. P. O'Donnell, K. M. Lee, and G. D. Watkins, J. Phys. C **16**, L723 (1983).
[20]M. Godlewski, W. E. Lamb, and B. C. Cavenett, J. Lumin. **24/25**, 173 (1981).
[21]G. Roussos, J. Nagel, and H. J. Schulz, J. Phys. B **53**, 97 (1983).